The impact of bond dissociation energyp and electron withdrawing on metastable phase control mechanism in copper selenides

OR

Deconvoluting the mechanisms behind copper selenide formation from diaryl diselenide precursors

Alexandra C. Koziel[❖], Janet E. Macdonald[*,†,❖]

❖Department of Chemistry and †Vanderbilt Institute for Nanoscale Science and Engineering, Vanderbilt University, Nashville, Tennessee 37235, United States

Abstract:

To tailor specific applications of copper selenide, the ability to systematically differentiate between the stable and metastable phases and understand the mechanisms behind these different formations is imperative. Here, we use ^{1}H, ^{13}C, ^{77}Se NMR, STA, and XRD to develop and examine the activity and decomposition of selenium precursors in a copper selenide nanoparticle synthesis. The multitude of techniques help clarify the relationships between solvent, precursor, temperature, and metals. Finally, through these unique nanoparticle characterization techniques, we show that active selenium radicals play a major role in copper selenide phase control. This work exemplifies the unique tools that can be used to examine and illuminate the mysteries within nanoparticle synthesis.

Background:

The ability to control phase in semiconductor nanocrystals remains a predominantly mysterious process, and yet being able to selectively synthesize one phase over another is integral to the success of inorganic materials in many technologies.

In binary and ternary materials, there are often phases of several stoichiometries as well as polymorphic pairs. For examples, the copper selenides contain eight phases and colloidal syntheses to many of these phases have been reported.[1] The connections between these reports are often opaque. What is truly controlling the phase of the product? Is it the rate at which one or

more of the reagents react? Is it the chemical potential of one or more of the precursors? Several publications have detailed the path to thermodynamic and metastable phases using kinetic studies[2–6] to analyze the effects of the substituent groups on the reagents and bond dissociation energy (BDE) publications[7–9] that look at how the different precursors' bond energies affect the resulting nanoparticles (NPs).

But often ignored is *how* the precursors break down which has an underappreacited role in phase control. For example, we found synthetically that a decomposition mechanism specific to diallyl disulfide in the presence of alkyl amines was key to the formation of iron pyrite over other iron sulfides. Additionally, Hollingsworth *et al*. showed how changing the solvent from OLAM to hexylamine changed the intermediate in their decomposition mechanism of nickel dithiocarbamates and thus affected phase.[10]

Particularly intriguing are the two reagents dibenzyl diselenide (Bn_2Se_2) and diphenyl diselenide (Ph_2Se_2) as they are known to give different phases in colloidal synthesis. The Brutchey group used a molecular programming approach and the contrasting BDEs of Bn_2Se_2 and Ph_2Se_2 to achieve unique metastable phases.[9] The Vela group observed zinc blende vs wurtzite polymorphism in CdSe using these two reagents, notably citing the difference in their BDE as a main contributing factor to the different phases.[8] The Schimpf group changed the ratios of precursors with different reactivities, including Ph_2Se_2, to synthesize new heterostructures of WSe_2.[11] Finally, the Schaak group found that at high temperatures for short times (220-250ºC under 30 min) a new weisseite-like ($Cu_{2-x}Se$) phase forms from the reaction of Ph_2Se_2, $Cu(acac)_2$, and OLAM before forming berzelianite ($Cu_{2-x}Se$).[12]

While Bn_2Se_2 and Ph_2Se_2 have structural similarities, these two reagents have very distinct chemistries. Phenyl groups are more electron donating toward the Se than benzyl

groups.[13] Additionally, benzyl groups have an aliphatic $–CH_2$ that the phenyl does not allowing for distinct chemistries and reactivities. Ph_2Se_2 has a weaker Se—Se bond compared to its C—Se bond, conversely Bn_2Se_2 has a weaker C—Se bond compared to its Se—Se bond which should lead to differing radical based chemisty.[9] These variations in chemistry should lead to unique phase control and decomposition trends.

Lardon *et al.* used ^1H NMR to study the decomposition mechanism of neat diaryl diselenides,[14,15] finding decomposition products including selenides, triselenides and other organic byproducts. [14,15] What is not known is how the presence of Lewis bases, such as primary amines or Lewis Acids in the form of metal ions might influence this chemistry.

The copper chalcogenides are important targets because of their uses in thermo- and opto-electronics, applications which could be potentially improved upon with the use of the novel metastable phases, which are rare and difficult to synthesize.[8,9,19–21] One notable study has evaluated the mechanism of copper sulfide (CuS) synthesis, but their studies did not include phase control.[22] In a similar system (copper selenide), the thermodynamic product is cubic, while the metastable one is hexagonal, but it is difficult to evaluate the mechanisms behind these syntheses.[23] This serendipity inspired the need for complete mechanistic understanding of nanoparticle synthesis.

It is of great interest to build off of these works to explore a project that analyzes the effects of decomposition products of diaryl diselenides on the phase of nanoparticles.[15,22] Through these studies knowledge will be acquired that allows for further tunability of nanoparticle phase leading to more pin pointed uses in applications.

This paper introduces a complete decomposition mechanism for the synthesis of copper selenide from diaryl diselenides (Bn_2Se_2 and Ph_2Se_2) and links the resulting active selenide products to phase control. Previous nanocrystal mechanism explorations using NMR have been done by the Hens group.[24–26] Their research has given the nanocrystal community an NMR toolbox for characterization of nanoparticle surfaces.[26,27] With the abilities of NMR in mind, Bn_2Se_2 and Ph_2Se_2 were strategically chosen for this study as they give access to ^{1}H, ^{13}C, and ^{77}Se NMR and have well defined BDEs through published DFT studies.[8,28] These methods were the backbone of the study into the decomposition of these precursors.

~~The above precursors have been used to study copper selenide phase control before, but never from a mechanistic point of view.[8,9] By heating these reagents up to classically high nanoparticle synthesis temperatures and analyzing the resulting products, a mechanism was composed. The effect of the active selenium precursors was linked to phase control. Ultimately, Ph_2Se_2 resulted in one phase, while Bn_2Se_2 resulted in three due the differing BDE's and electron withdrawing properties of these two precursors.~~

Methods: Diaryl diselenides were loaded into standard NMR tubes in an inert glove box and capped with a septa. They were then covered in a layer of parafilm preceding heating in a high heating oil bath between 140ºC-220ºC. A nitrogen balloon was inserted to prevent gas buildup. After 20-90 min the reactions were taken off, injected with deuterated solvent, and NMR was taken. Reactions with OLAM and copper(II) oleate were also run and are detailed in the supplemental information.

Results and Discussion

Importance of Bond Dissociation Energy

To understand the effect of bond dissociation energy (BDE) we looked to data from Tappan *et al.* that showed the Se—Se bond in Ph_2Se_2 is weakest (42.10 kCal/mol), while the C—Se bond is

weakest in Bn_2Se_2 (43.09 kCal/mol).[9] Due to these differences, unique products arose from each respective solo decomposition. We chose to use a 1:1 mole ratio of our diselenide precursors, OLAM, and copper(II) oleate as it led to more diverse phase trends and did not overwhelm to NMR signal.

The Ph_2Se_2 stayed intact until elevated temperature (220ºC, 50 min) at which point a signal arose in the ^{77}Se NMR (δ = 416 ppm) indicative of the formation of Ph_2Se. There was also Ph_2Se signal in the ^{1}H NMR at lower temperatures (200ºC). It is likely that the noisy baseline of the ^{77}Se baseline hid the signal and thus it did not appear until it was stronger. At even longer times of 90 min at 220°C, ^{77}Se NMR signals at δ = 562 and δ = 472 ppm were observed which can be assigned to Ph_2Se_3. [36, 39–414,29–31] Even though the signal had decreased, the most dominant selenium species in solution remained that of the starting material, Ph_2Se_2, even after 90 minutes at 220°C. This result is unsurprising as it is known that diselenides, when heated, form mixtures of polyselenides.[15] For Ph_2Se_2, the polyselenide chemistry was seen to be active above 220°C. Others have suggested that carbon-based radicals are important intermediates in the decomposition of selenides to other polyselenides.[15] Specifically, Lardon *et al.* suggested a radical mechanism for Ph_2Se_3 formation.[15] To investigate these radicals, TEMPO was added to our experiment to trap any intermediate radicals and confirm this hypothesis.[32] ^{1}H and ^{77}Se NMR indicated that the TEMPO trapped PhSe, rather than phenyl (see supporting information for detailed discussion of this assignment). The Se—Se bond is therefore homolytically cleaved at these elevated temperatures, consistent with the calculations that the Se—Se bond is weaker than the C—Se bond for Ph_2Se_2. Since a carbon-based radical was not trapped, we propose instead standard two electron chemistry is most important in the formation of the polyselenides, Ph_2Se_x. Radical chemistry involving $PhSe^{\cdot}$ is a possible active species in non-neat conditions.

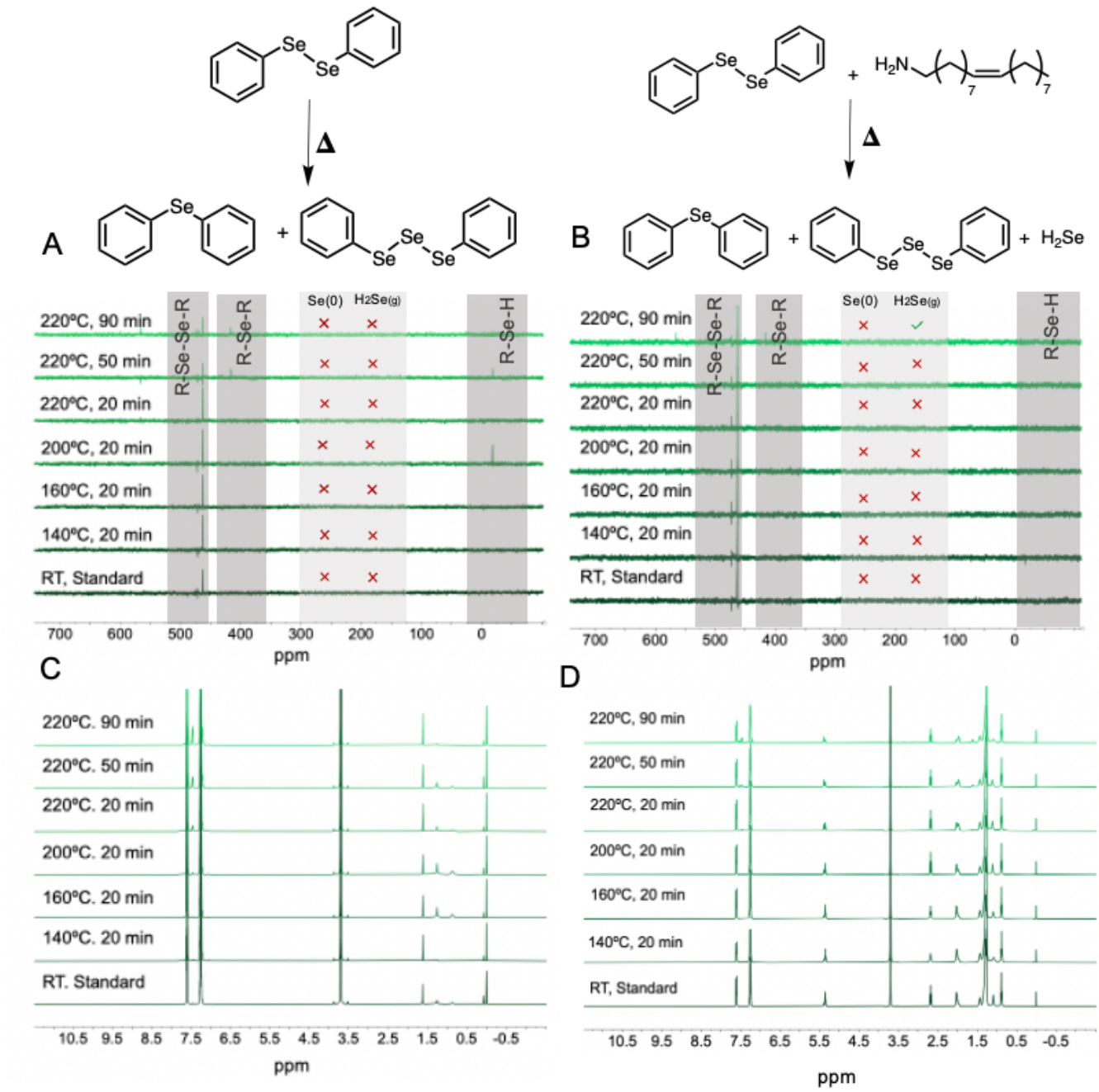

Figure 4. Each respective starting material was heated neat and with OLAM at the above temperatures and times to investigate the effects of the selenium precursor and common nanocrystal ligand. Dioxane standard at 3.17 ppm at 0.08 M. A) ^{77}Se NMR of Ph_2Se_2 B) ^{77}Se NMR of Ph_2Se_2 and OLAM C) ^{1}H NMR of Ph_2Se_2 D) ^{1}H NMR of PH_2Se_2 and OLAM. Presence of $H_2Se_{(g)}$ was analyzed by a lead acetate paper test shown in figure S5.

Dibenzyl Diselenide (Bn_2Se_2)

Bn_2Se_2 is less stable than Ph_2Se_2 as significant decomposition was observed at 160°C, 40ºC cooler than for the Ph_2Se_2. The selenium decomposition products were like that of Ph_2Se_2: Bn_2Se_3 (^{77}Se NMR δ = 538 and 410 ppm) Bn_2Se (δ = 331 ppm), and unreacted Bn_2Se_2 (δ = 410 ppm) but also included selenium metal (identified by XRD). The organic byproduct toluene was observed to form at temperatures above 200ºC as shown by the characteristic ^{1}H NMR peak at δ = 2.36 ppm corresponding to the CH_3.[30]

Contrary to Ph_2Se_2, the C—Se bond in Bn_2Se_2 is weaker than the Se—Se bond by 10.22 kCal/mol[9] and radical decomposition pathways are active for Bn_2Se_2 under neat conditions. The C—Se bond will break first in the Bn_2Se_2 mechanism resulting in a benzyl radical and a benzyl diselenide radical. Benzyl radicals scavenge H from the starting material and form toluene. Additionally, there is precipitation of selenium nanoparticles at temperatures above 160°C (the solution turned brown, and the precipitate analyzed by XRD), followed by the formation of bulk metallic selenium as a pellet at 220°C (mp 221ºC [33]). It is likely that the remaining BnSeSe· radical is prone to the loss of Se(0) and the formation of a second Bn•. In addition, similar to the Ph_2Se_2, the polyselenide chemistry is active at 200°C.

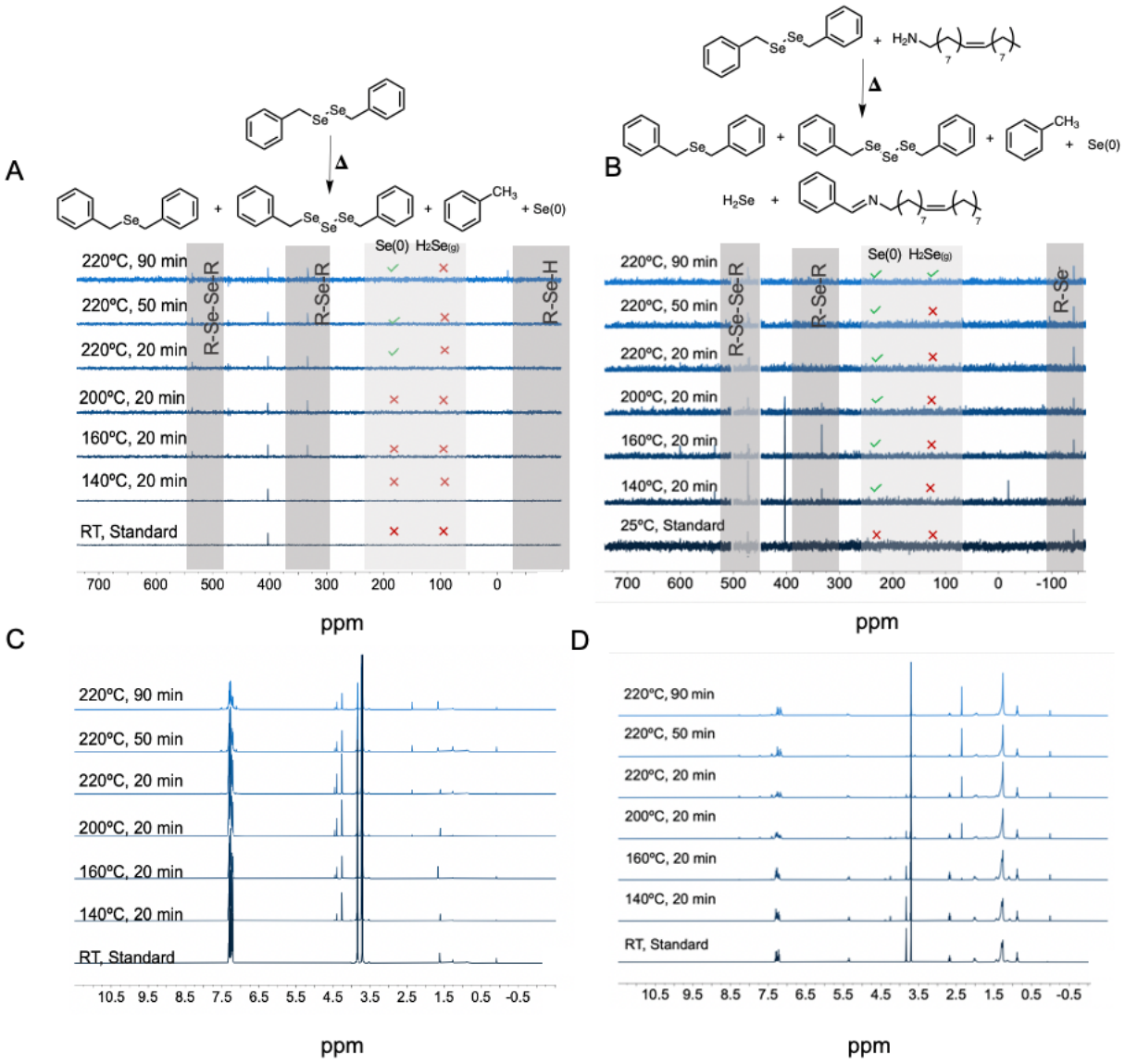

Figure 5. To understand the effects of the Bn_2Se_2 and OLAM NMR studies were run at the above temperatures and times. A) ^{77}Se NMR of Bn_2Se_2 B) ^{77}Se of Bn_2Se_2 and OLAM C) ^{1}H NMR of Bn_2Se_2 D) ^{1}H NMR of Bn_2Se_2 and OLAM.

The Importance of Amines in the formation of H_2Se

The *in situ* production of $H_2Se_{(g)}$ and $H_2S_{(g)}$ have precedent in the synthesis of nanocrystalline metal sulfide and selenides.[7,22,34–37] The Krauss group, interested in the mechanisms in CdSe QD synthesis, used ^{77}Se to show that $H_2Se_{(g)}$ was a byproduct at 250ºC when tri-n-butylphosphine

selenide was injected into octanoic acid in tetradecane.[36] Additionally, the Ozin group studied the "*Oleylamine-Sulfur Black Box"* and showed that upon heating OLAM and elemental sulfur to 130ºC, $H_2S_{(g)}$ formed with evidence from the shifts ^{1}H NMR and the darkening of lead acetate indictor paper in the reaction headspace. The study proposed that the formation of thioamine intermediates release an equivalent of $H_2S_{(g)}$, which then reacts in the presence of excess amine to form an amidine and another equivalent of $H_2S_{(g)}$. The study proposed that the reactions to form $H_2S_{(g)}$ affected the production of copper sulfide NPs by acting as a sulfur precursor.[22] Therefore, $H_2Se_{(g)}$ is a possible product of the decomposition products Ph_2Se_2 and Bn_2Se_2 especially in the presence of amines such as OLAM. OLAM provides a plethora of hydrogens for abstraction by Se based radicals for the production of $H_2Se_{(g)}$.[38,39]

Using lead acetate indicator paper placed in the head space of the reactions, the production of $H_2Se_{(g)}$ was tested. Neat, neither Bn_2Se_2 nor Ph_2Se_2 released $H_2Se_{(g)}$ when heated to 220°C, yet it was produced in both cases when the OLAM was present.

Ph_2Se_2 and OLAM

When Ph_2Se_2 decomposes in the presence of OLAM, the ^{77}Se NMR indicated the same polyselenide products seen under neat conditions at similar temperatures. It can be concluded the amine has little effect on the polyselenide chemistry described above.

However, the route to the new $H_2Se_{(g)}$ formation above 160°C must be considered. The ^{1}H NMR showed the formation of a new byproduct that includes signals in the aromatic (δ = 7.53 ppm) and aliphatic regions (δ = 1.6 ppm, 3.7 ppm) (supporting information), but we were not able to identify the structure(s). It can be concluded however, that $H_2Se_{(g)}$ is only formed from the scavenging of hydrogens from OLAM.

Bn_2Se_2 and OLAM

When Bn_2Se_2 and OLAM are mixed, changes are seen even at room temperature. The amine promotes the rotational isomerization of the diselenide leading to a splitting in the Se NMR (δ = 475, 476 ppm).[40] Decomposition products were observed at temperatures as low as 140°C, which was the lowest for any combination studied. Bn_2Se_3 and Bn_2Se formed at similar temperatures to neat conditions, but then were consumed much more readily as the temperatures increased with OLAM present. With time and heating, the signals of the Bn_2Se_2, Bn_2Se and, Bn_2Se_3 all decreased and disappeared, and benzylselenoate, $BnSe^-$, (^{77}Se NMR δ = -113 ppm) formed. The formation of Se(0) also occurred as low as 140°C. OLAM seems to promote the radical decomposition routes of Bn_2Se_2.

There are several pieces of evidence that OLAM is chemically active and is a source of hydrogen in the radical mechanisms. First, the amine and methylene ^{1}H NMR R—CH_2—NH_2 signals of OLAM (δ = 2.7 ppm and δ =1.08 ppm respectively) decrease in intensity and disappear while the terminal –CH_3 OLAM stays constant (compared to the dioxane standard). Second, the presence of amine greatly increased the production of toluene. By comparing the integrations of the –CH_3 ^{1}H NMR signal of toluene between the neat Bn_2Se_2 decomposition and the Bn_2Se_2 with OLAM, there is 17x more toluene produced when OLAM was present (when comparing to a dioxane standard). The increase in toluene is approximately commensurate with the loss in the amine signals noted above. This drastic increase in toluene production when the OLAM is present provides evidence that the OLAM donates hydrogens to radicals in solution.

Interestingly benzyl-cyano-oleate could be identified by ^{1}H NMR (δ = 7.8 and 8.3 ppm) as a minor product.[41] This is intriguing because this product suggests that the methylene protons of the phenyl group are the also donors for $H_2Se_{(g)}$ and possibly toluene formation, in addition to amine of OLAM as Ozin *et al.* had observed for sulfur in amines.[42]

Copper (II) Oleate Promotion

To confirm that the NMR tube conditions adequately modeled the more common nanocrystal synthesis conditions, "large scale" syntheses were performed to check that the resultant nanocrystal phases were similar. It was found that the systems are similar, however large scale syntheses progress further into marcasite- and pyrite-like (**supplemental information_____**).

Copper(II) Oleate and the decomposing.

Based on the decomposition studies (**schemes ___ and ____)** it was clear a plethora of selenium and organic decomposition products were forming. How does copper(II) oleate affect these decomposition products? Does copper play an active role in the selenium decomposition chemistry, or is it independent? A second series of NMR scale reactions were performed with the presence of copper(II) oleate and the diselenides with and without added OLAM. After the reactions, deuterated acetone was employed as the solvent to precipitate the resultant copper selenide nanoparticles from solution prior to NMR analysis.

For reactions of Ph_2Se_2 with copper(II) oleate (no OLAM), ^{77}Se NMR reveals the Ph_2Se_2 disappeared as Ph_2Se appeared, suggesting one selenium from Ph_2Se_2 is used for copper selenide formation. At very high temperatures of 220°C, the signal from Ph_2Se also began to decrease in intensity suggesting that high temperatures are needed for the selenoether to become reactive. Unlike the neat conditions, no Ph_2Se_3 was seen as a byproduct, thus the polyselenide is also very active in losing selenium for copper selenide production. Without copper, Ph_2Se was only seen after extensive heating at 220°C, whereas the Ph_2Se begins to form at only 160°C in the presence of copper. It can be concluded, that removal of Se from Ph_2Se_2 is promoted by copper and is part of the rate determining step.

With OLAM, the products and temperatures were similar as to when no amine was present. From this, we concluded that the amine has little effect on the relevant oragno-selenium decomposition chemistry of Ph_2Se_2 in the synthesis of copper selenides.

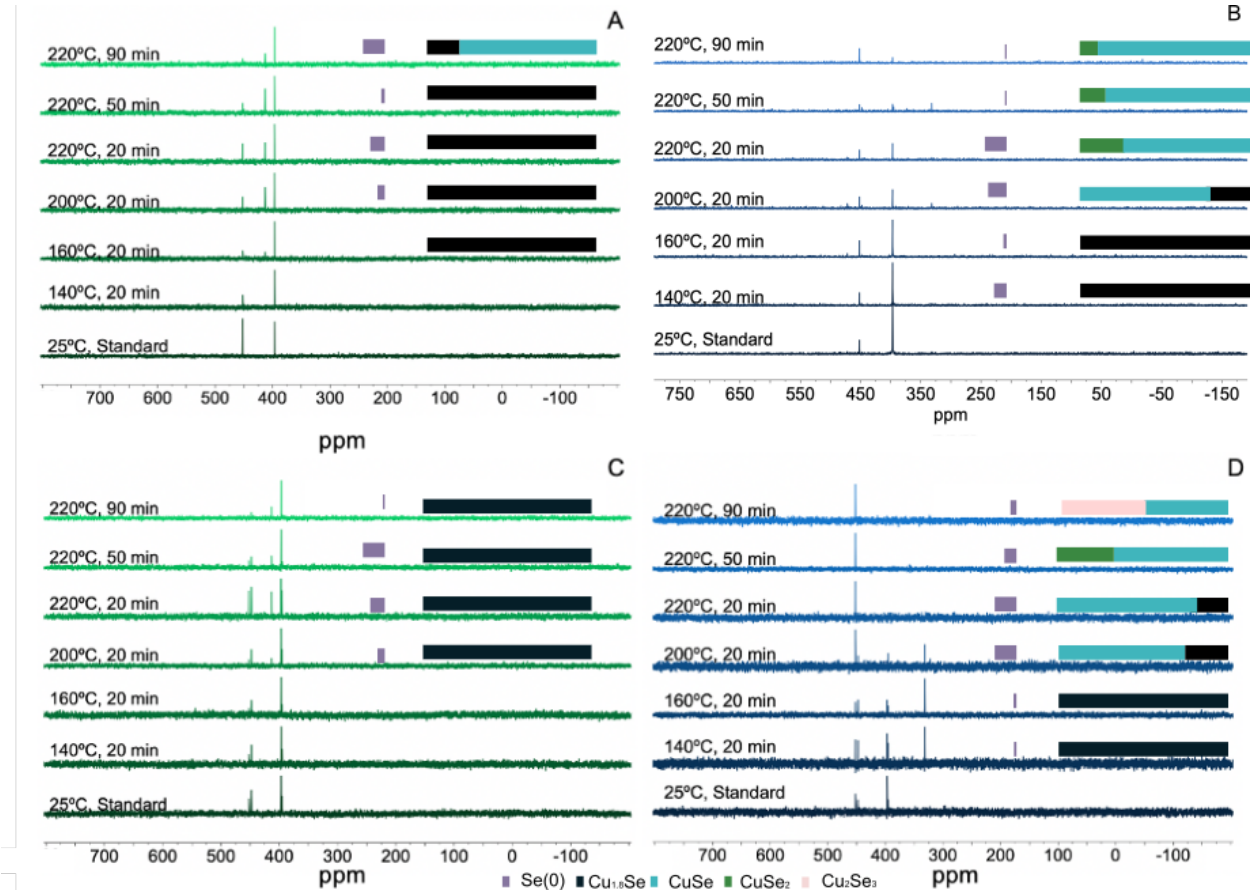

Figure___. ^{77}Se NMR of (a) Ph_2Se_2 and copper(II) oleate, (b) Bn_2Se_2 and copper(II) oleate, (c) Ph_2Se_2, OLAM, and copper(II) oleate. For each Ph_2Se_2 reach, one equivalent of Bn_2Se_2 (^{77}Se NMR δ = 410 ppm) was added to the NMR tube after heating as an internal standard. Correspondingly, each Bn_2Se_2 reactions contains a Ph_2Se_2 (^{77}Se NMR δ = 475 ppm) internal standard. These are normalized to 1. Times and temperatures without phase compositions did not produce nanoparticles or had starting material in the XRD pattern preventing accurate refinements.

Bn_2Se_2, OLAM, and Copper (II) Oleate

When Bn_2Se_2 was reacted with copper(II) oleate in the presence of OLAM, similar reactivity was seen to Ph_2Se_2; the selenoether forms as an intermediate, indicating a sequential

loss of selenium from the dichalcogenide precursor. This process occurred at 200°C for Ph_2Se_2, while Bn_2Se_2 began to lose the first Se at only 140°C.

For both Ph_2Se_2 and Bn_2Se_2, the presence copper lowers the temperature at which changes in the NMR occur compared to conditions without copper (Figure 3), indicating that copper is involved in the rate determining step for selenium loss. All reactions that went through the sequential loss of Se, were consistently contaminated by Se(0) either as nanoparticles or as pellet in the bottom of the reaction flask at all reaction temperatures. Without copper, (Figure xx) only in one case was Se(0) observed (Bn_2Se_2 neat at 220°C). The presence of copper therefore promotes the loss of Se from Ph_2Se_2 and Bn_2Se_2 to form Se(0) as well as the formation of copper selenides.

We look to the organometallic Chan-Lam coupling mechanism for selenoether formation to give clues as to how copper promotes the decomposition of the diselenides. The Chan-Lam mechanism can occur in the presence of Cu(I) or Cu(II) and contains radical additions of Ar_2Se_2 to give Ar-Se-Cu features as intermediates. The couplings are performed in the presence aryl boronic acids, which undergo transmetalation to give Cu-Ar features.[43] Reductive elimination of these two moieties yield the product selenoether. Here, without the presence of the boronic acid, we propose that alkyl migration at high temperatures from the Ar-Se-Cu leads to the needed Cu-Ar features for selenoether formation. The alkyl migration also gives "aryl-free" Se bound to copper which would lead to copper selenide formation. The Chan-Lam coupling to give selenoethers is not facile: it requires high catalysts loadings, and 100°C temperatures for 7 to 30 h. It is no surprise then that 140°C to 200°C is needed for this even more challenging decomposition and selenoether formation.

Bn_2Se_2 and Copper (II) Oleate

A completely different decomposition path was observed for Bn_2Se_2 without the presence of OLAM. Here, no Bn_2Se formation was observed and instead, the starting material was completely consumed at 140°C. A series of reactions at even lower temperatures (Supporting information) were not able to catch a selenoether intermediate, and only starting material (<140°C) or complete consumption (<160°C) was observed. Therefore, an entirely different and more facile mechanism over the Chan-Lam mechanism of decomposition occurs in this case. The presence of amine seems to shut down this special decomposition mechanism that the copper.

One of the challenges is that metal-organoselenium chemistry is under-studied compared to sulfur and oxygen, and so the more studied chalcogenides are needed provide mechanistic inspiration. Copper(II) is known to decompose peroxide to H_2O and O_2 for example. This first step is an equilibrium of Cu^{2+} to $[CuOOH]^+$, breaking the weak H-O bond.[44] We suggest that similar chemistry is occurring here with BnSeSeBn, where the Bn-Se bond is weak, and Cu-SeSeBn readily forms.[8,9] This beginning step would explain why both Se of Bn_2Se_2 are directly used to produce selenium(0) and copper selenides, and no triselenides or selenoethers were observed to form as intermediates. A catalytic decomposition could also be the source of the observed Se(0) seen at low temperatures.

The catalytic peroxide-like decomposition requires very specific conditions: weak R-Se bonds (Bn, not Ph) and non-reducing conditions (no amines). Amines at modest temperatures of ~100°C or even lower reduce Cu(II) to Cu(I), precluding the peroxide decomposition chemistry. Under the reducing conditions, only the Chan-Lam like chemistry at elevated temperature was available to Bn_2Se_2.[45]

Mechanism and phase control

For Ph_2Se_2, berzelianite($Cu_{1.8}Se$) formed at temperature >140°C along with a Se(0) and Ph_2Se. At the very highest temperature of 220°C and extended heating for 90 min, more selenium-rich klockmannite (CuSe) also formed, with a concomitant decrease in the Se(0) (8% at 50 min down to 0.8% at 90 min, supporting information), suggesting that the formation of klockmannite precludes Se(0) formation. The transformation also corresponds to the loss of Ph_2Se ^{77}Se NMR signal. It can be concluded that berzelianite($Cu_{1.8}Se$) formed through direct reaction of the copper(II) oleate with the Ph_2Se_2 reagent to give the Ph_2Se, whereas the secondary transformation of the berzelianite ($Cu_{1.8}Se$) to klockmannite (CuSe) occurred through reaction with the selenoether. We considered that the transformation of berzelianite ($Cu_{1.8}Se$) to klockmannite could originate from a reaction with Se(0), but it will be shown shortly that the temperature at which the transformation occurs is precursor dependent, excluding this interpretation. The formation of klockmannite(CuSe) was prevented by the presence of OLAM, suggesting strong surface stabilization that prevents a reaction with the reluctant Ph_2Se.

For Bn_2Se_2 in the presence of OLAM, at 140°C and 160°C the products formed were berzelianite ($Cu_{1.8}Se$), Se(0) and Bn_2Se. At 200°C and above, klockmannite (CuSe) also was observed. ^{77}Se NMR indicates a contemporaneous disappearance of Bn_2Se at this temperature. Again, this suggests that the formation of klockmannite (CuSe) occurs through the reaction of berzelianite($Cu_{1.8}Se$) and the Bn_2Se. This transformation occurs at less forcing conditions (lower temperature and shorter times) than the Ph_2Se, because the benzyl groups are more electron donating than phenyl groups. As mentioned before, this temperature dependance suggests that Se(0) is not the active reagent for the berzalianite($Cu_{1.8}$ Se) to klockmannite (CuSe) transition.

After heating at 220°C for 20 min, both the organic precursors Bn_2Se_2 and Bn_2Se were completely consumed to give mostly klockmannite (CuSe) with some remaining

berzelianite($Cu_{1.8}Se$) and Se(0). Extended heating for 50 min caused the further and complete consumption of the berzelianite($Cu_{1.8}Se$) to give klockmannite (CuSe), but also krutaite ($CuSe_2$). Additionally, the Se(0) impurity decreased in portion from ~26% down to 2%. It is likely that this further transformation to the most selenium-rich phase is caused by reaction with the Se(0) (possibly facilitated by OLAM). While there was some orthorhombic marcacitic *m*-$CuSe_2$, the dominant $CuSe_2$ phase was the high pressure cubic pyritic, krutaite (*p*-$CuSe_2$). Previous solid state reactions have shown that reactions of Na_2Se_2 and $CuCl_2$ over 6 weeks form the marcacitic phase (7 mol%), unless a small amount of water causes the intermediate formations of CuSe and Se(0). It was the reaction of CuSe and Se(0) that yielded the pyritic phase of *p*-$CuSe_2$.[46] Here we obtain similar results, but in a bottom up-reaction, under much shorter time frames and without the addition of water.

Even further heating of the reaction of Bn_2Se_2, copper(II) oleate and OLAM at 220°C for 90 min, saw that loss of the krutaite (CuSe2) and some of the klockmannite (CuSe) to yield a portion of umanginte (Cu_2Se_3). Umangite (Cu_2Se_3) has an intermediate selenium content compared to klockmannite and krutaite, suggesting a ripening to a more stable species. Solid state decompactions of *p*-$CuSe_2$ give Cu_2Se and CuSe instead, and so we conclude that the OLAM is important in stabilizing the umangite phase.

When in the presence of OLAM, Bn_2Se_2 goes through the Chan-Lam mechanism of decomposition, through a selenoether. In contrast, without OLAM, the facile peroxide-like decomposition occurs. At temperatures below 160ºC, berzelianite is the only product with some Se(0) impurity, but the balance of selenium remains as the Bn_2Se_2 precursor. At 200°C the promotes decomposition became rapid and a large amount of Se(0) was observed. The more Se rich klockmannite (CuSe) became the dominant copper selenide species over the more selenium-

poor berzelianite ($Cu_{1.8}Se$). Because the transformation of Berzalinaite ($Cu_{1.8}Se$) to Klockmanite (CuSe) happens at 200°C for Bn_2Se_2 but at 220°C with extended heating for Ph_2Se_2, we continue to think that this transformation does not occur though reaction with Se(0) but rather though direct reaction with the organometallic precursors. However, in this case, of Bn_2Se_2 with no OLAM present, the reaction is with the diselenide, rather than the selenoether.

At 200°C, the incorporation of selenium into a copper selenide becomes even more facile. No more berzelianite was observed, but only klockmannite (CuSe) and a small amount of pyritic krutaite (*p*-$CuSe_2$). With extended heating, the unstable krutaite ($CuSe_2$) decomposed, however umangite (Cu_2Se_3) was not the product as was seen when OLAM was present (see above). This is further evidence that OLAM is crucial to the stabilization of umangite.

The Brutchey group often uses a combination of Cu(II) oleate and Ph_2Se_2 in the presence of excess OLAM (as the solvent) at 220°C to yield umangite.[28,47] Under our conditions, the OLAM is limiting and umangite was not observed, instead only berzelianite was seen. We only observed umangite as a disproportionation between Cu_2Se and CuSe at temperatures above 220°C, and only when OLAM was present. Interestingly, solid state chemists have noticed that Cu_3Se_2 decomposed to $Cu_{2-x}Se$ and CuSe at only 135°C.[48] Therefore we must conclude, that OLAM provides such a strong surface ligation, that it actually changes the reaction equilibria to umangite.

Diphenyl Diselenide and Copper(II) oleate

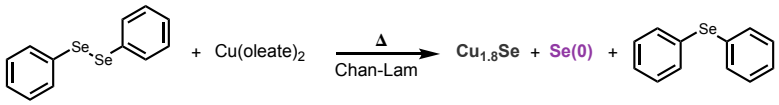

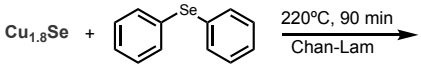

Diphenyl Diselenide, Copper(II) oleate, and OLAM

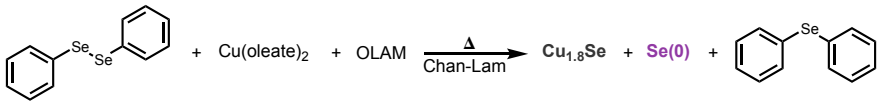

Dibenzyl Diselenide and Copper(II) oleate

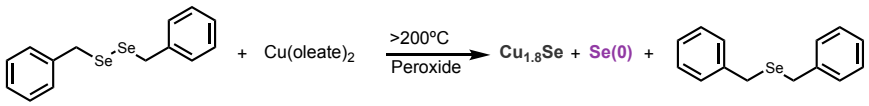

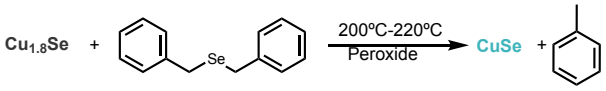

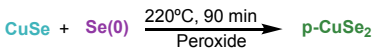

Dibenzyl Diselenide, Copper(II) oleate, and OLAM

Mechanisms from above dibenzyl diselenide and copper(II) oleate +

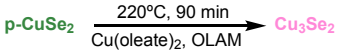

Conclusion

When precursors are heated to traditionally high NP synthesis temperatures they break down into organic and inorganic pieces that are ultimately dictated by their BDE. We found more reactive precursors (Bn_2Se_2) lead to more facile decomposition and metastable phases. Additionally, studies with OLAM proved that solvents and ligands are not always inert as gases such as $H_2Se(g)$ can arise and play a role in reactions.

Only the Bn_2Se_2 precursor led to a metastable product when mixed with OLAM and copper (II) oleate due to its weaker C—Se bond allowing it to be promoted by the copper (II) oleate. Future studies will pursue syntheses and mechanism analysis with additional diselenides precursors to further cement this trend. Overall, these mechanisms will lead to advancement of phase control

and can be built upon with different precursors and metal systems to gain understanding of more diverse systems. It is also very important to remember is that the metal was involved in the key decomposition steps, and so moving to other metal centers may cause yet again changes in decomposition mechanism and the chemical potential of the selenium precursors.

We attempted to gain more insight into the decomposition products of this reaction using a myriad of techniques including electron paramagnetic resonance (EPR), atmospheric pressure chemical ionization (APC), electrospray ionization (ESI), and gas chromatography (GC). With each of these techniques we faced barriers—there was no signal in the EPR, our starting material did not show strong absorption with APC, the compounds did not ionize for ESI, and the precursors decomposed on the GC column. The Ozin group attempted comparable methods in their metal sulfide blackbox study and found similar results.[42] It was therefore concluded that due to the very diagnostic ability of NMR the decomposition mechanisms could be determined from this single technique.

Author Information:
Corresponding Author
*J. E. Macdonald. Email: janet.macdonald@vanderbilt.edu

ORCID
Alexandra C. Koziel: 0000-0001-7960-9588
Janet E. Macdonald: 0000-0001-6256-0706

Notes:
The authors declare no competing financial interest.

Acknowledgements:
The authors would like to thank Donald Stec, PhD for help with NMR experimental setup. This project is based on work funded by the National Science Foundation (603057).

Works Cited:

(1) Guglielmi, Y.; Cappa, F.; Avouac, J. P.; Henry, P.; Elsworth, D. Seismicity Triggered by Fluid Injection-Induced Aseismic Slip. *Science (80-.).* **2015**, *348* (6240), 1224–1226. https://doi.org/10.1126/science.aab0476.

(2) Campos, M. P.; Hendricks, M. P.; Beecher, A. N.; Walravens, W.; Swain, R. A.; Cleveland, G. T.; Hens, Z.; Sfeir, M. Y.; Owen, J. S. A Library of Selenourea Precursors to PbSe Nanocrystals with Size Distributions near the Homogeneous Limit. *J. Am. Chem. Soc.* **2017**, *139* (6), 2296–2305. https://doi.org/10.1021/jacs.6b11021.

(3) Hendricks, M. P.; Cossairt, B. M.; Owen, J. S. The Importance of Nanocrystal Precursor Conversion Kinetics: Mechanism of the Reaction between Cadmium Carboxylate and Cadmium Bis(Diphenyldithiophosphinate). *ACS Nano* **2012**, *6* (11), 10054–10062. https://doi.org/10.1021/nn303769h.

(4) Hall, C. D.; Tweedy, B. R.; Kayhanian, R.; Lloyd, J. R. *The Kinetics and Mechanism of the Reaction of Tricoordinate Phosphorus Compounds with Diary1 Trisulfides*; 1992; Vol. 2.

(5) Martinolich, A. J.; Neilson, J. R. Toward Reaction-by-Design: Achieving Kinetic Control of Solid State Chemistry with Metathesis †. **2016**. https://doi.org/10.1021/acs.chemmater.6b04861.

(6) Rhodes, J. M.; Jones, C. A.; Thal, L. B.; MacDonald, J. E. Phase-Controlled Colloidal Syntheses of Iron Sulfide Nanocrystals via Sulfur Precursor Reactivity and Direct Pyrite Precipitation. *Chem. Mater.* **2017**, *29* (19), 8521–8530. https://doi.org/10.1021/acs.chemmater.7b03550.

(7) Guo, Y.; Alvarado, S. R.; Barclay, J. D.; Vela, J. Shape-Programmed Nanofabrication: Understanding the Reactivity of Dichalcogenide Precursors. *ACS Nano* **2013**, *7* (4), 3616–3626. https://doi.org/10.1021/nn400596e.

(8) Tappan, B. A.; Barim, G.; Kwok, J. C.; Brutchey, R. L. Utilizing Diselenide Precursors toward Rationally Controlled Synthesis of Metastable CuInSe2 Nanocrystals. *Chem. Mater.* **2018**, *30* (16), 5704–5713. https://doi.org/10.1021/acs.chemmater.8b02205.

(9) Lardon, M. A. *NMR Studies of Substituent Effects in Diphenyl Diselenides and of Thermally Induced Rearrangements in Dibenzyl Diselenide*; Rochester, NY, 1972.

(10) Lardón, M. Selenium and Proton Nuclear Magnetic Resonance Measurements on Organic Selenium Compounds. *J. Am. Chem. Soc. Soc.* **1970**, *92* (17), 5063–5066.

(11) Birchall, T.; Gillespie, R. J.; Vekris, S. L. Nuclear Magnetic Resonance Spectroscopy of Some Selenium Compounds. *Can. J. Chem.* **1965**, *43* (6), 1672–1679. https://doi.org/10.1139/v65-221.

(12) Chu, J. Y. C.; Lewicki, J. W. Thermal Decomposition of Bis(Diphenylmethy 1) Diselenide. *J. Org. Chem.* **1977**, *42* (14), 2491–2493.

(13) Geisenhoff, J. Q.; Tamura, A. K.; Schimpf, A. M. Manipulation of Precursor Reactivity for the Facile Synthesis of Heterostructured and Hollow Metal Selenide Nanocrystals. *Chem. Mater.* **2020**, *32* (6), 2304–2312. https://doi.org/10.1021/acs.chemmater.9b04305.

(14) Liu, H.; Owen, J. S.; Alivisatos, A. P. Mechanistic Study of Precursor Evolution in Colloidal Group II-VI Semiconductor Nanocrystal Synthesis. *J. Am. Chem. Soc.* **2007**, *129* (2), 305–312. https://doi.org/10.1021/ja0656696.

(15) Steckel, J. S.; Yen, B. K. H.; Oertel, D. C.; Bawendi, M. G. On the Mechanism of Lead Chalcogenide Nanocrystal Formation. *J. Am. Chem. Soc.* **2006**, *128* (40), 13032–13033.

https://doi.org/10.1021/ja062626g.

(16) Bullen, C.; Van Embden, J.; Jasieniak, J.; Cosgriff, J. E.; Mulder, R. J.; Rizzardo, E.; Gu, M.; Raston, C. L. High Activity Phosphine-Free Selenium Precursor Solution for Semiconductor Nanocrystal Growth. *Chem. Mater.* **2010**, *22* (14), 4135–4143. https://doi.org/10.1021/cm903813r.

(17) Brutchey, R. L. Diorganyl Dichalcogenides as Useful Synthons for Colloidal Semiconductor Nanocrystals. *Acc. Chem. Res.* **2015**, *48*, 2918–2926. https://doi.org/10.1021/acs.accounts.5b00362.

(18) Gilić, M.; Petrović, M.; Ćirković, J.; Paunović, N.; Savić-Sević, S.; Nikitović, Ž.; Romčević, M.; Yahia, I.; Romčević, N. Low-Temperature Photoluminescence of CuSe2 Nano-Objects in Selenium Thin Films. *Process. Appl. Ceram.* **2017**, *11* (2), 127–135. https://doi.org/10.2298/PAC1702127G.

(19) Hernández-Pagán, E. A.; Robinson, E. H.; La Croix, A. D.; MacDonald, J. E. Direct Synthesis of Novel Cu2- XSe Wurtzite Phase. *Chem. Mater.* **2019**, *31*, 4619–4624. https://doi.org/10.1021/acs.chemmater.9b02019.

(20) Tappan, B. A.; Brutchey, R. L. Polymorphic Metastability in Colloidal Semiconductor Nanocrystals. *ChemNanoMat*. John Wiley & Sons, Ltd August 24, 2020, pp 1567–1588. https://doi.org/10.1002/cnma.202000406.

(21) Thomson, J. W.; Nagashima, K.; MacDonald, P. M.; Ozin, G. A. From Sulfur-Amine Solutions to Metal Sulfide Nanocrystals: Peering into the Oleylamine-Sulfur Black Box. *J. Am. Chem. Soc.* **2011**, *133* (13), 5036–5041. https://doi.org/10.1021/ja1109997.

(22) Robinson, E. H.; Turo, M. J.; Macdonald, J. E. Controlled Surface Chemistry for the Directed Attachment of Copper(I) Sulfide Nanocrystals. *Chem. Mater.* **2017**, *29* (9),

3854–3857. https://doi.org/10.1021/acs.chemmater.6b05080.

(23) Hens, Z.; Martins, J. C. A Solution NMR Toolbox for Characterizing the Surface Chemistry of Colloidal Nanocrystals. *Chemistry of Materials*. 2013, pp 1211–1221. https://doi.org/10.1021/cm303361s.

(24) De Roo, J.; Yazdani, N.; Drijvers, E.; Lauria, A.; Maes, J.; Owen, J. S.; Van Driessche, I.; Niederberger, M.; Wood, V.; Martins, J. C.; et al. Probing Solvent-Ligand Interactions in Colloidal Nanocrystals by the NMR Line Broadening. *Chem. Mater.* **2018**, *30* (15), 5485–5492. https://doi.org/10.1021/acs.chemmater.8b02523.

(25) Tappan, B. A.; Barim, zde; Kwok, J. C.; Brutchey, R. L. Utilizing Diselenide Precursors toward Rationally Controlled Synthesis of Metastable CuInSe 2 Nanocrystals. *Chem. Mater* **2018**, *30*, 40. https://doi.org/10.1021/acs.chemmater.8b02205.

(26) Gladysz, J. A.; Hornby, J. L.; Garbe, J. E. A Convenient One-Flask Synthesis of Dialkyl Selenides and Diselenides via Lithium Triethylborohydride Reduction of Sex. *J. Org. Chem.* **1978**, *43* (6), 1204–1208. https://doi.org/10.1021/jo00400a040.

(27) Fulmer, G. R.; Miller, A. J. M.; Sherden, N. H.; Gottlieb, H. E.; Nudelman, A.; Stoltz, B. M.; Bercaw, J. E.; Goldberg, K. I. NMR Chemical Shifts of Trace Impurities: Common Laboratory Solvents, Organics, and Gases in Deuterated Solvents Relevant to the Organometallic Chemist. *Organometallics* **2010**, *29* (9), 2176–2179. https://doi.org/10.1021/om100106e.

(28) Eggert, H.; Nielsen, O.; Henriksen, L. 77Se NMR. Application of Se-Se to the Analysis of Dialkyl Polyselenides. *J. Am. Chem. Soc.* **1986**, *108* (8), 1725–1730. https://doi.org/10.1021/ja00268a001.

(29) Bowry, V. W.; Ingold, K. U. Kinetics of Nitroxide Radical Trapping. 2. Structural Effects.

J. Am. Chem. Soc. **1992**, *114* (13), 4992–4996. https://doi.org/10.1021/ja00039a006.

(30) Teng, Q.-H.; Yao, Y.; Wei, W.-X.; Tang, H.-T.; Li, J.-R.; Pan, Y.-M. Direct C–H Sulfenylation of Quinoxalinones with Thiols under Visible-Light-Induced Photocatalyst-Free Conditions. *Green Chem.* **2019**, *21*, 6241. https://doi.org/10.1039/c9gc03045j.

(31) Duddeck, H.; Wagner, P.; Rys, B. 77Se,13C And1H NMR Spectra of Acyclic Phenylselenenylalkanes and -Alkenes and Some of Their Selenoxides. *Magn. Reson. Chem.* **1993**, *31* (8), 736–742. https://doi.org/10.1002/mrc.1260310809.

(32) Bianco, C. L.; Akaike, T.; Ida, T.; Nagy, P.; Bogdandi, V.; Toscano, J. P.; Kumagai, Y.; Henderson, C. F.; Goddu, R. N.; Lin, J.; et al. The Reaction of Hydrogen Sulfide with Disulfides: Formation of a Stable Trisulfide and Implications for Biological Systems. *Br. J. Pharmacol.* **2019**, *176* (4), 671–683. https://doi.org/10.1111/bph.14372.

(33) Cai, Y.-R.; Hu, C.-H. Computational Study of H 2 S Release in Reactions of Diallyl Polysulfides with Thiols. **2017**. https://doi.org/10.1021/acs.jpcb.7b03683.

(34) Seo, Y. H.; Jo, Y.; Choi, Y.; Yoon, K.; Ryu, B. H.; Ahn, S.; Jeong, S. Thermally-Derived Liquid Phase Involving Multiphase Cu(In,Ga)Se2 Nanoparticles for Solution-Processed Inorganic Photovoltaic Devices. *RSC Adv.* **2014**, *4* (35), 18453–18459. https://doi.org/10.1039/c4ra00623b.

(35) Henthorn, H. A.; Pluth, M. D. Mechanistic Insights into the H2S-Mediated Reduction of Aryl Azides Commonly Used in H2S Detection. *J. Am. Chem. Soc.* **2015**, *137* (48), 15330–15336. https://doi.org/10.1021/jacs.5b10675.

(36) Yordanov, G. G.; Yoshimura, H.; Dushkin, C. D. Phosphine-Free Synthesis of Metal Chalcogenide Quantum Dots by Means of in Situ-Generated Hydrogen Chalcogenides. *Colloid Polym. Sci.* **2008**, *286* (6–7), 813–817. https://doi.org/10.1007/s00396-008-1840-

z.

(37) Frenette, L. C.; Krauss, T. D. Uncovering Active Precursors in Colloidal Quantum Dot Synthesis. *Nat. Commun.* **2017**, *8* (1), 1–8. https://doi.org/10.1038/s41467-017-01936-z.

(38) Jung, Y. K.; Kim, J. Il; Lee, J. K. Thermal Decomposition Mechanism of Single-Molecule Precursors Forming Metal Sulfide Nanoparticles. *J. Am. Chem. Soc.* **2010**, *132* (1), 178–184. https://doi.org/10.1021/ja905353a.

(39) Hou, B.; Benito-Alifonso, D.; Webster, R.; Cherns, D.; Galan, M. C.; Fermín, D. J. Rapid Phosphine-Free Synthesis of CdSe Quantum Dots: Promoting the Generation of Se Precursors Using a Radical Initiator. *J. Mater. Chem. A* **2014**, *2* (19), 6879–6886. https://doi.org/10.1039/c4ta00285g.

(40) Hoyte, R. M.; Denney, D. B. Cis-Trans Isomerization of Allylic Radicals. *J. Org. Chem.* **1974**, *39* (17), 2607–2612. https://doi.org/10.1021/jo00931a035.

(41) Jain, V. K. Chapter 1. An Overview of Organoselenium Chemistry: From Fundamentals to Synthesis. In *Organoselenium Compounds in Biology and Medicine*; 2017; pp 1–33. https://doi.org/10.1039/9781788011907-00001.

(42) Munemori, D.; Tsuji, H.; Uchida, K.; Suzuki, T.; Isa, K.; Minakawa, M.; Kawatsura, M. Copper-Catalyzed Regioselective Allylic Cyanation of Allylic Compounds with Trimethylsilyl Cyanide. *Synthesis (Stuttg).* **2014**, *46* (20), 2747–2750. https://doi.org/10.1055/S-0034-1378322.

(43) Thomson, J. W.; Nagashima, K.; MacDonald, P. M.; Ozin, G. A. From Sulfur-Amine Solutions to Metal Sulfide Nanocrystals: Peering into the Oleylamine-Sulfur Black Box. *J. Am. Chem. Soc.* **2011**, *133* (13), 5036–5041. https://doi.org/10.1021/ja1109997.